

**Gain in three-dimensional metamaterials utilizing semiconductor quantum structures**

Stephan Schwaiger, Matthias Klingbeil, Jochen Kerbst, Andreas Rottler, Ricardo Costa, Aune Koitmäe, Markus Bröll, Christian Heyn, Yuliya Stark, Detlef Heitmann, and Stefan Mendach\*

*Institut für Angewandte Physik und Zentrum für Mikrostrukturforschung, Universität Hamburg, Jungiusstrasse 11, D-20355 Hamburg, Germany*

(Received 2 August 2011; revised manuscript received 6 October 2011; published 31 October 2011)

We demonstrate gain in a three-dimensional metal/semiconductor metamaterial by the integration of optically active semiconductor quantum structures. The rolling-up of a metallic structure on top of strained semiconductor layers containing a quantum well allows us to achieve a tightly bent superlattice consisting of alternating layers of lossy metallic and amplifying gain material. We show that the transmission through the superlattice can be enhanced by exciting the quantum well optically under both pulsed or continuous wave excitation. This points out that our structures can be used as a starting point for arbitrary three-dimensional metamaterials including gain.

DOI: [10.1103/PhysRevB.84.155325](https://doi.org/10.1103/PhysRevB.84.155325)

PACS number(s): 78.67.Pt, 42.70.-a, 78.60.Lc

**I. INTRODUCTION**

Metamaterials are composite materials made of artificial building blocks whose size and lattice constant is small compared to the wavelength of the transmitted light. An advantage of metamaterials compared to conventional natural materials is that their properties can be tailored by varying the size and shape of the artificial building blocks. In particular, using metallic structures, a negative index of refraction in the near-infrared and visible regime had been realized using metallic split ring resonators<sup>1</sup> or fishnet structures.<sup>2-4</sup> To prove bulk properties and use metamaterials for devices, one has to achieve a three-dimensional structure which is usually planar lithographically defined and fabricated sequentially until the desired thickness is reached.<sup>5-7</sup> These stacks of planar functional layers are usually classified as a three-dimensional metamaterial.<sup>5,7,8</sup> All these metamaterials are hampered by absorption, which is caused by ohmic losses in the metallic compound or, in other words, by the finite imaginary part of the dielectric function of the metal. A proposal to compensate these losses is to integrate a gain medium into the metamaterial, which amplifies the transmitted light<sup>9</sup> like, e.g., dye<sup>10</sup> or semiconductor quantum structures.<sup>11,12</sup> Recently it has been shown that a dye surrounding the metallic structures can compensate the losses in a metamaterial.<sup>13</sup> In contrast to dyes, semiconductor quantum structures exhibit no photo bleaching, a higher damage threshold, and the possibility of electrical pumping. Investigations on two-dimensional planar systems show that metallic structures can be coupled to a quantum structure and partially compensate the ohmic losses.<sup>14-16</sup>

In this paper, we present a multilayered radial metamaterial consisting of alternating layers of metal structures and amplifying semiconductor quantum structures. For the fabrication, we utilize the concept of self-rolling strained layers<sup>17-19</sup> which we recently extended to strained metal/semiconductor metamaterials with a possible application as a hyperlens.<sup>20-22</sup> Here we investigate a novel structure with active quantum wells integrated into the semiconductor layer. As a result, we obtain a three-dimensional metamaterial containing optical amplifiers which enhance the light transmission. We present transmission measurements which show a transmission enhancement of about 5% under optical continuous wave (cw)

excitation. Under pulsed excitation, a relative enhancement in transmission of 11% was measured. We can well model our data by transfer matrix calculations, and we use finite-difference time-domain simulations (FDTD) to illustrate the effect of gain on the functionality of a rolled-up hyperlens.

**II. STRUCTURES AND EXPERIMENTAL SETUP**

In Fig. 1(a), we present a sketch of our sample. Using molecular beam epitaxy (MBE), a GaAs buffer layer (500 nm) is grown on a GaAs substrate, followed by an AlAs sacrificial layer (40 nm), the strained lower barrier layer consisting of Al<sub>20</sub>In<sub>13</sub>Ga<sub>67</sub>As (23 nm), the quantum well consisting of In<sub>16</sub>Ga<sub>84</sub>As (7 nm), and finally the unstrained top barrier layer consisting of Al<sub>23</sub>Ga<sub>77</sub>As (21 nm). Subsequently the structure is metalized with Ag (13 nm) using thermal evaporation. By selective etching with HF, the sacrificial layer is removed, causing the strained layers to bend up while minimizing the strain energy. Microtubes with inner radii of about  $r_{\text{inner}} \approx 3-4 \mu\text{m}$  are formed. The walls of the microtubes represent superlattices of metallic and gain layers [Fig. 1(b)]. All radial dimensions are more than one order of magnitude smaller than the wavelength of the transmitted light  $\lambda > 894 \text{ nm}$ , fulfilling the criteria for an effective metamaterial, while the two other (roll axis and roll circumference) dimensions are mesoscopic.

To measure the change in transmission through the radial metamaterial we used a tapered optical fiber, which was metalized and structured using focused ion beams. Light from a tunable cw Ti:sapphire laser is coupled into the untapered end of the fiber. This fiber emits the laser light from a hole in the side wall of the tip perpendicular to its axis and acts as a “torch” [Fig. 2(a)] which can be placed inside a microtube [Fig. 2(b)]. The microtube and the fiber tip are located inside a flow cryostat and can be moved with respect to each other using an XYZ piezo cube (attocube systems). Either a frequency doubled Nd:YAG cw laser ( $E_{\text{cw}} = 2.33 \text{ eV}$ ) or a pulsed picosecond diode laser ( $E_{\text{pulse}} = 1.95 \text{ eV}$ ) can be focused with a spot size of  $A_{\text{spot}} \approx 4 \mu\text{m}^2$  onto the tube with a microscope objective [Fig. 2(d)]. The transmitted light as well as the photoluminescence (PL) from the quantum well are collected with the same objective, energetically filtered with a spectrometer, detected with a single photon counting module,

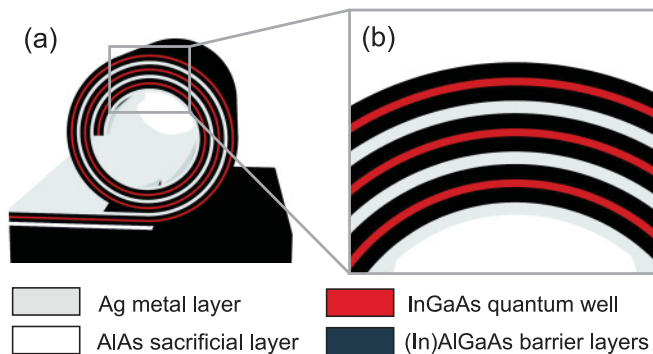


FIG. 1. (Color online) (a) A planar metal/semiconductor structure can be transformed into a three-dimensional metamaterial using the self-rolling concept of strained layers. (b) The wall of the microtube is a metamaterial with alternating metallic (Ag) and gain layers (InGaAs quantum well).

and acquired using a counter. For the measurements with the pulsed laser, a start-stop-electronic is set between the counting module to only count events within a range of  $\Delta t = 10$  ns around the laser pulse. The repetition rate of the laser was 1 MHz, and the nominal pulse width  $\tau_{\text{FWHM}} = 68$  ps. In order to keep the pulse shape constant, the power was adjusted by turning a lambda-half waveplate mounted between two

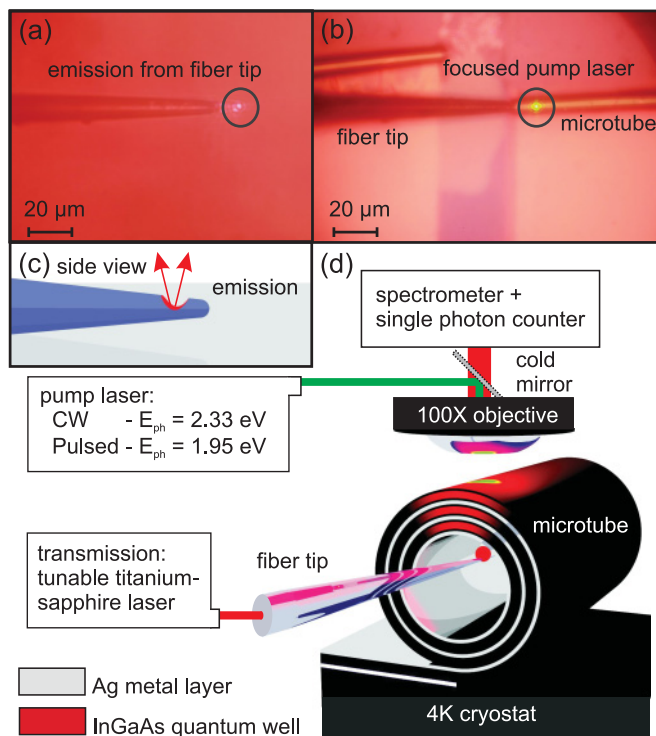


FIG. 2. (Color online) (a) Micrograph of a tapered optical fiber which is emitting light only from a spot on the side wall of the tip. (b) The fiber tip can be inserted into a microtube and illuminate it from the inside. To excite the quantum well in the tubes' wall, a pump laser can be focused onto the microtubes. (c) Sketch of the side view of the light emitting fiber. (d) To measure the transmission enhancement fiber and tube are located in a transmission setup. As a pump laser either a pulsed or a cw laser are used. Light from a tunable Ti:sapphire laser is fed into the fiber and allows the transmission measurement.

crossed polarization filters. Due to the complicated setup and our limited time resolution, the peak power and pulse shape are not well characterized when incident onto the microtube. Nevertheless, we also achieved valuable information from the pulsed measurements.

Since the transmitted light and the PL exhibit the same energy, we have to distinguish between transmission enhancement and PL as follows. Using an appropriate chopping system, we acquire at a frequency of 150 Hz the dark level ( $I_D$ ), the transmitted signal without pumping ( $I_T$ ), the PL without the fiber emitting light ( $I_{\text{PL}}$ ), and subsequently the transmitted signal along with the PL ( $I_{\text{TPL}}$ ). All these values are taken within one period, which allows very accurate measurements free from any long-term drift of the experimental setup. The relative transmission enhancement without PL:  $\frac{\Delta T}{T} = \left(\frac{I_{\text{TPL}} - I_{\text{PL}}}{I_T - I_D}\right) - 1$  is plotted in the following measurements versus the photon energy of the transmitted light with a standard deviation of each transmission value of  $\sigma\left(\frac{\Delta T}{T}\right) \approx 0.4\%$  and  $\sigma\left(\frac{\Delta T}{T}\right) \approx 0.8\%$  for the cw and the pulsed measurements, respectively. To achieve a spectrum, we scanned the energy of the tunable cw Ti:sapphire laser. The power emitted from the fiber tip was about  $P_{\text{E cw}} \approx 0.2$  nW for the cw measurements, and  $P_{\text{E pulse}} \approx 18$  nW for the pulsed measurements.

### III. RESULTS AND DISCUSSION

In Fig. 3(a), we present the transmission enhancement under cw excitation of a microtube which is rolled up three times. At a pump power  $P_{\text{cw}} = 34$   $\mu\text{W}$  [Fig. 3(a)], the transmission enhancement exhibits its maximum at  $E_T = 1.365$  eV. The maximum value is  $\frac{\Delta T}{T} = 4.6\%$  with respect to the transmission if the quantum well is not pumped. At higher photon energies, the transmission decreases toward its unpumped value. As will be discussed in more details later in the paper, the transmission is slightly negative  $\frac{\Delta T}{T} \approx -0.7\%$  at photon energies below  $E_T = 1.359$  eV. It increases again toward lower photon energies to its initial value.

The measured data can be confirmed by calculations using the transfer matrix method<sup>23</sup> with the dielectric function  $\epsilon$  for Ag<sup>24</sup> and GaAs.<sup>24</sup> According to Ref. 11, a Lorentz oscillator is added to the dielectric function of the semiconductor  $\epsilon_{\text{SC}}(\omega)$  to achieve the dielectric function of the gain layer  $\epsilon_{\text{Gainlayer}}(\omega)$ :

$$\epsilon_{\text{Gainlayer}}(\omega) = \epsilon_{\text{SC}}(\omega) + \left( \frac{A\omega_L^2}{\omega_L^2 - \omega^2 - i\omega\gamma_L} \right), \quad (1)$$

where  $A$  is an amplitude,  $\omega_L$  the central frequency of the quantum well, and  $\gamma_L$  a damping frequency of the quantum well. We express the amplitude  $A$  as a gain constant  $\alpha$ , which is the amplification per length, by the following equation:

$$\alpha = - \frac{A\omega_L^2}{\text{Re}(\sqrt{\epsilon_{\text{SC}}})c_0\gamma_L}, \quad (2)$$

where  $c_0$  is the speed of light. Unfortunately, in the present system we do not have the experimental opportunity to derive the absorption of the quantum well in the unpumped state. Therefore the calculated spectra of the pumped quantum wells were normalized to the transmission spectra with a gain constant of  $\alpha = 0$ .

The chosen Lorentz oscillator has its central energy at  $E_L = 1.364$  eV with a damping of  $\gamma_L = 6$  meV. The gain constant  $\alpha$  is

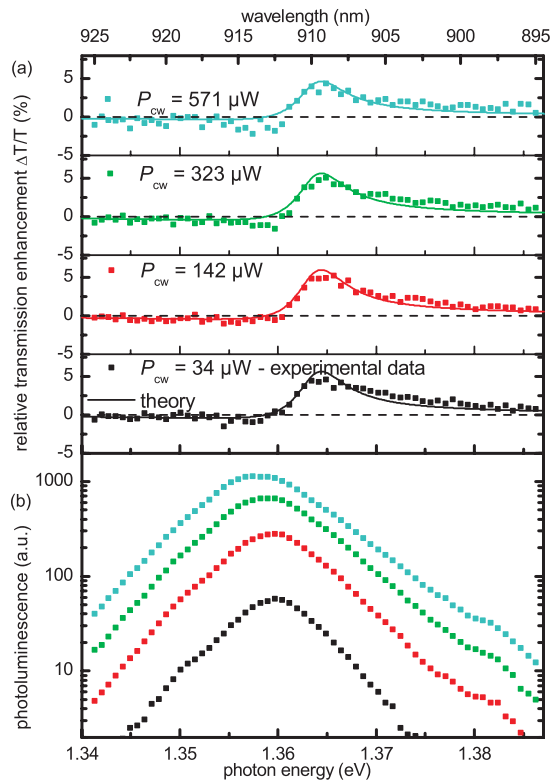


FIG. 3. (Color online) (a) Transmission enhancement spectra through the microtube under optical cw excitation at different pump powers (squares). At low pump powers (up to  $P_{cw} = 323 \mu\text{W}$ ) the enhanced transmission can be explained with a Lorentz oscillator model (solid lines). At high pump powers  $P_{cw} = 571 \mu\text{W}$  deviations from the model occur. (b) Corresponding PL data (squares). The PL exhibits a Lorentz shape. The peak position shifts to lower energy with increasing power due to the heating of the microtube.

fitted to each measurement. For the transmission enhancement at a power  $P_{cw} = 34 \mu\text{W}$ , we determine  $\alpha = 1700 \text{ cm}^{-1}$ . The corresponding PL is shown in Fig. 3(b). It exhibits its maximum at  $E_{PL} = 1.36 \text{ eV}$  in the vicinity of the Lorentz oscillators' central energy, indicating the quantum well as the origin of the transmission enhancement. The PL is red-shifted by 4 meV with respect to the central energy of the Lorentzian, which indicates the well-known Stokes-Shift of the PL.<sup>25</sup> At higher excitation powers, the PL increases in intensity and shifts to lower energies. At a power of  $P_{cw} = 571 \mu\text{W}$ , it is red-shifted by 2 meV with respect to the low pumping-powers measurements. This effect can be explained by the increasing heating of the microtube and the related bandgap shift.

To exclude possible heating effects, we also performed measurements with a pulsed laser which are shown in Fig. 4. At a power  $P_{av} = 0.28 \mu\text{W}$ , the shape of the transmission enhancement is comparable with the cw measurements. The corresponding calculations were performed with a gain constant of the Lorentz oscillator ( $\alpha = 1800 \text{ cm}^{-1}$ ). By increasing the power  $P_{av}$ , the maximum of the transmission enhancement increases and exhibits a value of  $\frac{\Delta T}{T} = 11.3\%$  at  $P_{av} = 2 \mu\text{W}$ . The corresponding gain constant is  $\alpha = 2800 \text{ cm}^{-1}$ . At excitation powers above  $P_{av} > 2 \mu\text{W}$ , the amplitude saturates at  $\alpha = (2780 \pm 130) \text{ cm}^{-1}$ . Even at the highest power,  $P_{av} = 11.4 \mu\text{W}$ , no significant deviation from the model is observed.

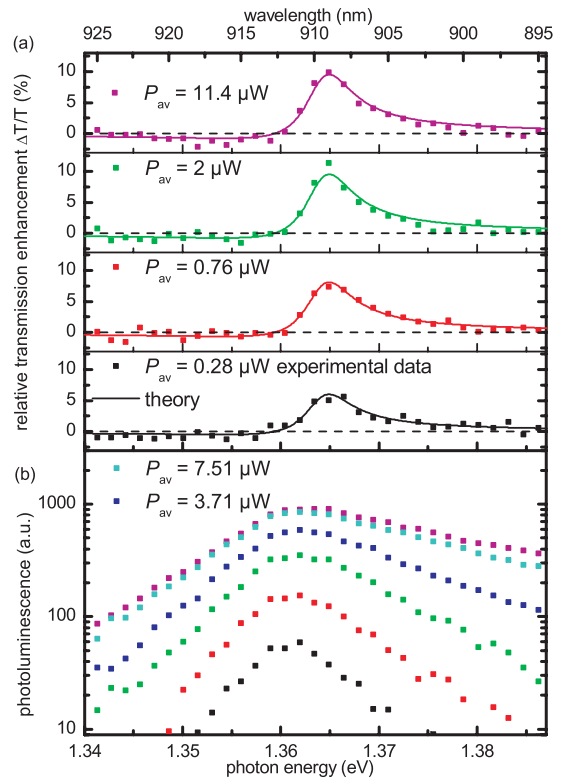


FIG. 4. (Color online) (a) Transmission enhancement spectra through the microtube under pulsed excitation at different pump powers (squares). Every measurement can be explained with the Lorentz oscillator model (solid lines) by assuming an increasing gain constant which saturates at  $P_{av} \approx 2 \mu\text{W}$ . (b) The corresponding PL (squares) exhibits no red-shift but a high energy tail at pump powers above  $P_{av} = 2 \mu\text{W}$ . This indicates that the lowest energy level in the quantum well is populated and stimulated emission occurs. For  $P_{av} = 3.71 \mu\text{W}$  and  $P_{av} = 7.51 \mu\text{W}$  only the PL data is shown.

This clearly shows that the transmission enhancement can be attributed to a change of the dielectric function of the quantum well itself.

In Fig. 4(b), we present the corresponding PL data. All curves exhibit their maximum at the same energetical position as in the low-power cw measurements [Fig. 3(b)  $P_{cw} = 34 \mu\text{W}$ ]. The PL signal under pulsed excitation first increases with power but then saturates at powers above  $P_{av} \approx 7.5 \mu\text{W}$ . A clear difference compared to the cw measurements is the high energy tail of the PL at high pump powers. We explain this tail by band filling effects. A similar behavior in planar In(Ga)As quantum wells was observed in Refs. 26 and 27. The band filling implies that the lowest energy levels are populated, and the quantum well exhibits stimulated emission. Filling of the lowest levels also explains the saturation of gain observed at  $P_{av} > 2 \mu\text{W}$  with pulsed excitation. The negative change in transmission in certain energy regimes, which is in the first moment surprising, can be attributed to a change of the dielectric function of the quantum well which changes the optical length of the metamaterial and therefore the Fabry-Pérot condition. The change in transmission in the high-power cw measurements ( $P_{cw} = 571 \mu\text{W}$ ) exhibits deviations from our model, because our model does not include heating effects. Using a pulsed laser

source, we excluded heating effects while increasing the peak power with respect to the power  $P_{cw}$  in the cw measurements.

In this paragraph, we discuss the influence of the optically active quantum wells on the absorption in the total multilayered system. Based on the derived gain constants and transfer-matrix calculations, we calculate the total absorption  $A$  of the three bilayers of Ag ( $d_{Ag} = 13$  nm) and GaAs ( $d_{GaAs} = 51$  nm). At an energy of  $E_T = 1.364$  eV, the absorption exhibits  $A \approx 20\%$ . By replacing the passive GaAs layer with an active GaAs gain layer ( $\alpha = 2800$  cm<sup>-1</sup>), we derive an absorption value for the total system of  $A \approx 16\%$ . Consequently the losses could be reduced but not overcome.

Rolled-up metal/semiconductor microtubes are promising candidates for the application as a rolled-up hyperlens. The curved structure exhibits an anisotropic permittivity with a component parallel  $\epsilon_p$  and perpendicular  $\epsilon_s$  to the single layers.<sup>28,29</sup> This anisotropic permittivity can lead to either an elliptical or hyperbolic dispersion. In the case of elliptical dispersion, the unidirectional propagation of light and subwavelength imaging occurs over a broad energy range if  $\epsilon_s$  is large and in particular  $\epsilon_s \gg \epsilon_p$ .<sup>21,22</sup> These conditions are fulfilled in the vicinity of the plasma frequency  $\omega_{\epsilon_p=0}$ . At the quantum wells emission energy of  $E_L = 1.364$  eV, our rolled-up microtube exhibits an elliptic dispersion with the effective permittivities of  $\epsilon_p = 2.6$  and  $\epsilon_s = 17.6$ . To illustrate the influence of the gain on the transmission through the rolled-up microtube, we show in Fig. 5(a) a FDTD simulation of the fabricated microtube. We placed two dipoles in a distance of 450 nm located at the inner perimeter of the microtube. The dipoles emit at an energy  $E_{dipole} = 1.364$  eV. The dimensions were chosen according to the fabricated microtubes [three layers of Ag ( $d_{Ag} = 13$  nm) and GaAs ( $d_{GaAs} = 51$  nm)] with an inner radius of  $r_{inner} = 3$   $\mu$ m. The gain constant of the GaAs layer was chosen according to the measurements  $\alpha = 2800$  cm<sup>-1</sup>. Although the magnification of this hyperlens exhibits only  $\frac{r_{outer}}{r_{inner}} \approx 1.1$ , it is visible that subwavelength details of the two dipole sources are transmitted through the microtube. By comparing this simulation with a simulation on a microtube with a passive semiconductor, we found that the spatial distribution of the electromagnetic fields only changes marginally while the total transmission increases by  $\frac{\Delta T}{T} = 8\%$ .

In order to examine the radial propagation of electromagnetic waves inside the rolled-up microtube in more detail, we performed a FDTD simulation of a rolled-up microtube with 11 rotations and the same single layer thickness [Ag ( $d_{Ag} = 13$  nm) and GaAs ( $d_{GaAs} = 51$  nm)]. The emission energy of the quantum well as well as the emission energy of the two dipoles are adapted to  $E_{dipole} = E_L = 1.212$  eV in order to match the effective plasma frequency  $\omega_{\epsilon_p=0}$  and therefore improve the unidirectional light propagation. The effective permittivity is now  $\epsilon_p = 0.04$  and  $\epsilon_s = 16.4$ . The gain constant of the GaAs layer was chosen again according to the measurements  $\alpha = 2800$  cm<sup>-1</sup>. Although the absorption in the metal layers is too high to be compensated by the quantum well, the simulation shows two cones emitted from the two dipoles penetrating into the material. In accordance with Ref. 20, the single layer thicknesses have to be reduced in order to optimize the operation as a rolled-up hyperlens.

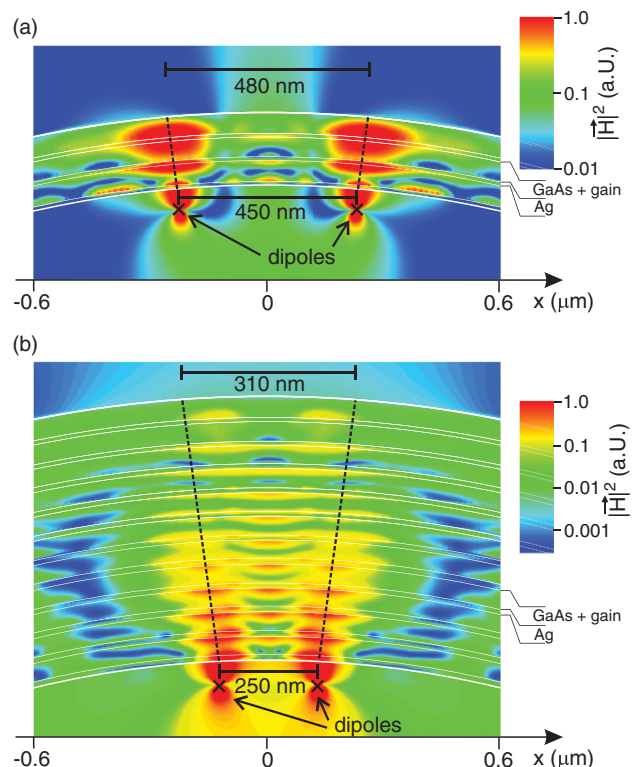


FIG. 5. (Color online) (a) FDTD simulation of the investigated rolled-up metal/semiconductor superlattice containing three alternating layers of Ag ( $d_{Ag} = 13$  nm) and optically active GaAs ( $d_{GaAs} = 51$  nm). The magnetic field intensity  $|H_z|^2$  is plotted color coded in logarithmic scale. Two dipoles are placed in a distance of 450 nm at the inner perimeter of the microtube. The electromagnetic waves emitted from the dipoles  $E_{dipole} = 1.364$  eV are transmitted through the superlattice. (b) By performing a simulation with 11 layers of Ag ( $d_{Ag} = 13$  nm) and optically active GaAs ( $d_{GaAs} = 51$  nm) we examine the propagation of electromagnetic waves inside the material. The emission energy of the quantum well and the dipoles are  $E_{dipole} = E_L = 1.212$  eV. The light is strongly damped inside the materials but nevertheless radially channelled.

#### IV. CONCLUSION

In conclusion, we showed that using the concept of self-rolling we can fabricate a three-dimensional metamaterial. Our rolled-up metamaterial contains several alternating layers of metal and robust semiconductor gain material while maintaining the effective medium approximation. Although we did not reach transparency of the material, we demonstrated a transmission enhancement of  $\frac{\Delta T}{T} = 4.6\%$  and  $\alpha = 1700$  cm<sup>-1</sup> under cw excitation of the embedded quantum well. For pulsed excitation, we found  $\frac{\Delta T}{T} = 11\%$  and  $\alpha = 2800$  cm<sup>-1</sup>. The latter values are so far limited by our experimental time resolution. The actual transmission enhancement might be higher if extracted from measurements with higher time resolution. Furthermore we illustrated the influence of gain for the example of a rolled-up hyperlens. In the next step, the concept opens the road to utilize plasmonic resonances in three-dimensional metamaterials consisting of metallic nanostructures sandwiched between gain layers.

## ACKNOWLEDGMENTS

The authors thank W. Hansen and C. Strelow for fruitful discussions, and A. Stemmann for MBE sample growth. We

gratefully acknowledge support from the Universität Hamburg and the Deutsche Forschungsgemeinschaft (DFG) through GrK 1286.

\*smendach@physnet.uni-hamburg.de

- <sup>1</sup>S. Linden, C. Enkrich, M. Wegener, J. Zhou, T. Koschny, and C. M. Soukoulis, *Science* **306**, 1351 (2004).
- <sup>2</sup>G. Dolling, C. Enkrich, M. Wegener, C. M. Soukoulis, and S. Linden, *Opt. Lett.* **31**, 1800 (2006).
- <sup>3</sup>G. Dolling, M. Wegener, C. M. Soukoulis, and S. Linden, *Opt. Lett.* **32**, 53 (2007).
- <sup>4</sup>S. Xiao, U. K. Chettiar, A. V. Kildishev, V. P. Drachev, and V. M. Shalaev, *Opt. Lett.* **34**, 3478 (2009).
- <sup>5</sup>N. Liu, H. Guo, L. Fu, S. Kaiser, H. Schweizer, and H. Giessen, *Nat. Mater.* **7**, 31 (2007).
- <sup>6</sup>Z. Liu, H. Lee, Y. Xiong, C. Sun, and X. Zhang, *Science* **315**, 1686 (2007).
- <sup>7</sup>J. Valentine, S. Zhang, T. Zentgraf, E. Ulin-Avila, D. A. Genov, G. Bartal, and X. Zhang, *Nature (London)* **455**, 376 (2008).
- <sup>8</sup>H. O. Moser and C. Rockstuhl, *Laser Photonics Rev.* (2011), doi:10.1002/lpor.201000019.
- <sup>9</sup>S. Anantha Ramakrishna and J. B. Pendry, *Phys. Rev. B* **67**, 201101 (2003).
- <sup>10</sup>M. A. Noginov, G. Zhu, M. Bahoura, J. Adegoke, C. E. Small, B. A. Ritzo, V. P. Drachev, and V. M. Shalaev, *Opt. Lett.* **31**, 3022 (2006).
- <sup>11</sup>A. A. Gomyadinov, V. A. Podolskiy, and M. A. Noginov, *Appl. Phys. Lett.* **91**, 191103 (2007).
- <sup>12</sup>Z.-G. Dong, H. Liu, T. Li, Z.-H. Zhu, S.-M. Wang, J.-X. Cao, S.-N. Zhu, and X. Zhang, *Appl. Phys. Lett.* **96**, 044104 (2010).
- <sup>13</sup>S. Xiao, V. P. Drachev, A. V. Kildishev, X. Ni, U. K. Chettiar, H.-K. Yuan, and V. M. Shalaev, *Nature (London)* **466**, 735 (2010).
- <sup>14</sup>P. Vasa, R. Pomraenke, S. Schwieger, Y. I. Mazur, V. Kunets, P. Srinivasan, E. Johnson, J. E. Kihm, D. S. Kim, E. Runge, G. Salamo, and C. Lienau, *Phys. Rev. Lett.* **101**, 116801 (2008).
- <sup>15</sup>E. Plum, V. A. Fedotov, P. Kuo, D. P. Tsai, and N. I. Zheludev, *Opt. Express* **17**, 8548 (2009).
- <sup>16</sup>N. Meinzer, M. Ruther, S. Linden, C. M. Soukoulis, G. Khitrova, J. Hendrickson, J. D. Oritzky, H. M. Gibbs, and M. Wegener, *Opt. Express* **18**, 24140 (2010).
- <sup>17</sup>V. Y. Prinz, V. A. Seleznev, A. K. Gutakovsky, A. V. Chehovskiy, V. V. Preobrazhenskii, M. A. Putyato, and T. A. Gavrilova, *Physica E* **6**, 828 (2000).
- <sup>18</sup>O. G. Schmidt and K. Eberl, *Nature (London)* **410**, 168 (2001).
- <sup>19</sup>O. Schumacher, S. Mendach, H. Welsch, A. Schramm, C. Heyn, and W. Hansen, *Appl. Phys. Lett.* **86**, 143109 (2005).
- <sup>20</sup>S. Schwaiger, M. Bröll, A. Krohn, A. Stemmann, C. Heyn, Y. Stark, D. Stickler, D. Heitmann, and S. Mendach, *Phys. Rev. Lett.* **102**, 163903 (2009).
- <sup>21</sup>E. J. Smith, Z. Liu, Y. F. Mei, and O. G. Schmidt, *Appl. Phys. Lett.* **95**, 083104 (2009).
- <sup>22</sup>E. J. Smith, Z. Liu, Y. F. Mei, and O. G. Schmidt, *Appl. Phys. Lett.* **96**, 019902 (2010).
- <sup>23</sup>M. Born and E. Wolf, *Principles of Optics* (Pergamon Press, Oxford, 1980).
- <sup>24</sup>E. D. Palik, *Handbook of Optical Constants of Solids* (Academic Press, New York, 1985).
- <sup>25</sup>G. Bastard, C. Delalande, M. H. Meynadier, P. M. Frijlink, and M. Voos, *Phys. Rev. B* **29**, 7042 (1984).
- <sup>26</sup>S. Marcinkevicius, G. Ambrazevicius, T. Lideikis, and K. Naudzius, *Solid State Commun.* **79**, 889 (1991).
- <sup>27</sup>E. Tournie, O. Brandt, and K. Ploog, *Appl. Phys. A* **56**, 109 (1993).
- <sup>28</sup>B. Wood, J. B. Pendry, and D. P. Tsai, *Phys. Rev. B* **74**, 115116 (2006).
- <sup>29</sup>Z. Jacob, L. V. Alekseyev, and E. Narimanov, *Opt. Express* **14**, 8247 (2006).